MANUSCRIPT Scientific Services...
www.manuscriptscientific.com

Journal of Oral Health and Dentistry Research
(ISSN: 2583-522X)

Case Report Open Access

Intraoral Scan-Based Documentation of Interimplant Papilla Reconstruction with a Tunneled Pediculated Connective Tissue Graft After Anterior Maxillary Trauma: A Clinical Report

Bruno Viana Reis[1, 2*], Victor Vidigal[2], Fillipe Marcone dos Santos Dutra[2], Renan Lana Devita[1,2]

[1]*Royal College of Surgeons in Ireland*

[*2]*Unique Dental, Dublin, Ireland.*

Corresponding author: Bruno Viana Reis, Unique Dental, 90-97 Cork Street, Dublin, Ireland, D08R6KX. Email: brunoviana@rcsi.ie. Phone: +353 83 477 3446. ORCID: 0009-0004-2747-7535.

Abstract

Reconstruction of an interimplant papilla in the anterior maxilla remains challenging when trauma has destroyed the buccal plate and soft-tissue scaffold. This clinical report describes staged rehabilitation of traumatic loss of teeth 11 and 12 in a 38-year-old man using implant-supported restorations, prosthetic contour modification, a tunneled palatal pediculated connective tissue graft for papilla reconstruction, and a second connective tissue graft for buccal contour augmentation.

Serial intraoral scans were acquired at baseline (T0), before tissue-grafting (T1), and after healing (T2). Scans were processed in CloudCompare using a registration workflow based on stable posterior and premolar anatomy after exclusion of the treated anterior region. The final buccal region of interest extended from the distal aspect of tooth 13 to the distal aspect of tooth 22. Surface change was documented with C2M signed distances and directional 2.5D surface-change indicators.

The interimplant papilla between implants 11 and 12 improved from Jemt papilla index score 0 at T1 to score 3 at T2. Buccal ROI analysis showed cumulative outward surface displacement from T0 to T2, with a mean C2M signed distance of +1.281 mm, a median of +0.896 mm, and 96.33% positive values. The clinically relevant X-projection indicator increased from +23.626 mm3 for T0-T1 to +283.495 mm3 for T0-T2. This report supports serial IOS documentation as a non-ionising method for visualising peri-implant soft-tissue surface changes, while not replacing direct biological volumetric measurement.

Keywords: Anterior Maxilla; Intraoral Scanning; Interimplant Papilla; Connective Tissue Graft; Digital Surface Analysis.

INTRODUCTION

Aesthetic rehabilitation after anterior maxillary trauma requires restoration of missing teeth, reconstruction of tissue contours, and creation of a prosthetic emergence profile that supports the peri-implant mucosa. These requirements are magnified when avulsion is associated with buccal plate fracture, because the loss of hard-tissue support can compromise both the vestibular contour and the interproximal soft-tissue architecture.

The interimplant papilla is especially difficult to reconstruct because adjacent implants do not provide the same periodontal vascular and anatomic support as adjacent natural teeth. Papillary fill is influenced by the vertical relationship between the contact point and the bone crest and by the horizontal distance between adjacent implants [1,2,8]. These relationships help explain why papilla reconstruction between two implants is less predictable than augmentation of buccal soft-tissue thickness alone.

Connective tissue grafting can improve peri-implant mucosal thickness and aesthetic stability, and soft-tissue phenotype modification has become a central component of implant therapy in the aesthetic zone [3,4,13,16]. However, traumatic defects often require a staged surgical-prosthetic approach, because prosthetic contours, implant positions, bone reconstruction, provisional tissue conditioning, and soft-tissue grafting must be coordinated.

Digital documentation has also become increasingly relevant. Serial intraoral scans provide a non-ionising method for recording external surface morphology, and scan superimposition can help visualise contour changes over time [5,18]. Nevertheless, longitudinal comparison is technique sensitive. If the treated region is used for registration, the alignment algorithm may partially adapt to the area that is expected to change and underestimate the true difference. Therefore, stable non-treated anatomy should be used preferentially for registration when the objective is to evaluate tissue change in the anterior maxilla.

Received: *September 12, 2026;* ***Revised:*** *September 14, 2026;* ***Accepted:*** *September 16, 2026*

Citation: Reis BV, Vidigal V, Santos Dutra FMD & Devita RL. (2026) Intraoral Scan-Based Documentation of Interimplant Papilla Reconstruction with a Tunneled Pediculated Connective Tissue Graft After Anterior Maxillary Trauma: A Clinical Report. J Oral Health Dent Res, 5(3): 1-14.

Copyright: ©2026 Reis BV, Vidigal V, Santos Dutra FMD & Devita RL. This is an open-access article distributed under the terms of the Creative Commons Attribution License, which permits unrestricted use, distribution, and reproduction in any medium, provided the original author and source are credited.

This clinical report has two objectives. The first is to present an alternative surgical-prosthetic approach for reconstructing a deficient interimplant papilla between adjacent implants after severe anterior maxillary trauma. The second is to describe a practical intraoral-scan and CloudCompare workflow for processing the images and documenting soft-tissue surface changes and directional 2.5D surface-change indicators.

CLINICAL REPORT

A 38-year-and-7-month-old male patient presented after severe anterior maxillary trauma. Emergency management before referral included wound cleansing, removal of debris, facial suturing, and splinting from tooth 13 to tooth 23 [17]. Clinical and radiographic evaluation showed avulsion of teeth 11 and 12, complicated crown fractures with pulpal exposure of teeth 21 and 22, and fracture of the buccal bone plate. Because the sockets and buccal plate were severely compromised, reimplantation of the avulsed incisors was not considered feasible. The treatment objectives were to restore the missing anterior teeth, maintain the fractured teeth when possible, reconstruct buccal and papillary soft-tissue volume, eliminate the interimplant black triangle, and document the dimensional changes with serial intraoral scans (**Figure 1**).

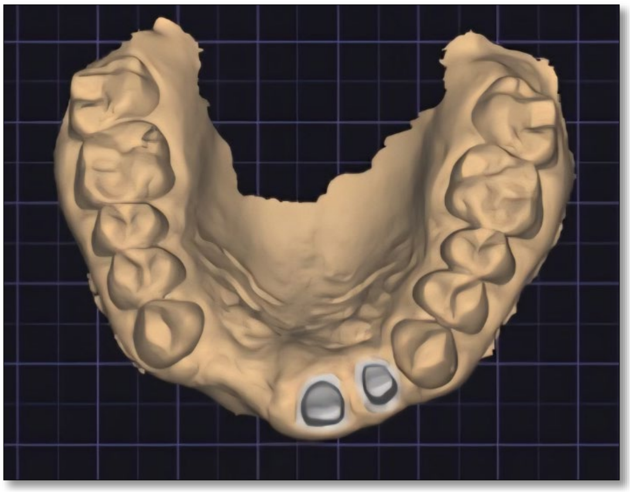

Figure 1. Initial clinical presentation. Preoperative intraoral aspect after severe anterior maxillary trauma, showing the compromised anterior maxillary region before definitive rehabilitation

Root canal treatment of teeth 21 and 22 was performed on 23 April 2024. Both canals were irrigated with sodium hypochlorite and EDTA, prepared with the ProTaper Gold system, and obturated with gutta-percha and Sealapex sealer. Digital prosthetic planning was performed by exporting an intraoral scan to Exocad software. Pre-trauma photographic information was used as an aesthetic reference for anterior tooth morphology, incisal edge position, smile curvature, and prosthetic planning (**Figure 2**).

On 2 May 2024, fibre posts were placed in teeth 21 and 22, followed by tooth preparation and delivery of a fixed provisional restoration. The provisional restoration was supported by teeth 21 and 22 and replaced teeth 11 and 12 as cantilever pontics. This prosthesis provided immediate aesthetic stabilization and functioned as a restorative reference for implant planning.

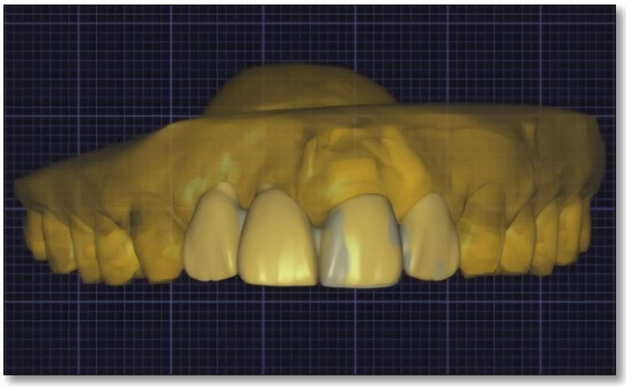

Figure 2. Digital planning and buccal contour assessment. Digital planning views used to evaluate anterior tooth arrangement, restorative contours, and the loss of buccal contour in the traumatic defect.

Implant surgery was performed in the regions of teeth 11 and 12 on 22 August 2024. Implant positions were planned from the restorative design, and a surgical guide was used to initiate the osteotomy sequence. The residual post-traumatic bone anatomy prevented complete execution of the digitally planned trajectories, so the final osteotomies were adjusted manually during surgery to engage the remaining native bone and obtain primary stability. Two tapered implants measuring 3.75 × 13 mm were placed in positions 11 and 12. Simultaneous guided bone regeneration was performed with particulate graft material and a membrane to augment the buccal defect, support implant coverage, and re-establish a ridge contour appropriate for soft-tissue conditioning.

After approximately 3 months of healing, the implants were reopened. On 21 November 2024, implant impressions were made, the original provisional restoration was replaced, individual provisional crowns were fabricated for teeth 21 and 22, and screw-retained provisional crowns were fabricated for implants 11 and 12. The implant-supported provisional crowns were used to condition the peri-implant mucosa and guide the emergence profiles. Although peri-implant soft-tissue maturation improved, a visible black triangle persisted between the implant crowns at positions 11 and 12.

The definitive ceramic crowns were delivered on 4 March 2025. The cervical and transmucosal regions of the implant-supported crowns were intentionally narrowed to reduce mucosal compression and create space for soft-tissue augmentation. This restorative decision was part of the reconstructive strategy, because the prosthesis was used to provide a protected volume into which grafted connective tissue could mature. Before soft-tissue reconstruction, the interimplant papilla between implants 11 and 12 was classified as Jemt score 0, indicating absence of papillary fill and a visible interimplant black triangle (**Figure 3, 4**).

Figure 3. Definitive crowns before soft-tissue reconstruction, frontal view. A visible interimplant black triangle persisted between implant-supported crowns 11 and 12 before soft-tissue grafting. The interimplant papilla was scored as Jemt 0 at this stage.

Figure 4. Definitive crowns before soft-tissue reconstruction, lateral view. The image demonstrates the prosthetic emergence profile and the residual buccal soft-tissue contour deficiency before grafting.

Soft-tissue reconstruction was performed on 13 May 2025. The main objective was to reconstruct the papilla between implants 11 and 12 while improving the broader buccal soft-tissue contour. A palatal donor area was prepared from approximately the mesial region of tooth 16 to the mesial region of tooth 13. A continuous connective tissue segment approximately 1.5 mm wide was de-epithelialized and sectioned while preserving its mesial attachment. This design maintained a pediculated vascular supply. A recipient tunnel was prepared internally through the peri-implant soft tissue from the vestibular aspect toward the palatal donor region. External vertical releasing incisions were avoided, and the external papillary envelope was preserved [14]. The pediculated connective tissue was rotated through the tunnel and positioned toward the vestibular interimplant papilla region to increase the three-dimensional connective tissue volume between implants 11 and 12 (**Figure 5**).

Figure 5. Soft-tissue grafting procedure. Occlusal view showing preparation and positioning of the palatal pediculated connective tissue graft used for interimplant papilla reconstruction.

A second free connective tissue graft was harvested from the contralateral palate, extending approximately from tooth 23 to the mesial region of tooth 26. This graft was de-epithelialized and positioned to augment the buccal contour across the anterior maxilla, particularly around implants 11 and 12. The two grafting components therefore addressed two related but different deficiencies: the interimplant papillary volume and the vestibular collapse caused by the original trauma. The tissues were stabilized with suspensory sutures to reduce tension and maintain graft position (**Figure 6**).

Figure 6. Soft-tissue grafting procedure. Frontal view showing buccal graft positioning and stabilization with suspensory/tension-reducing sutures to support the reconstructed papillary and buccal volume.

The patient was followed until 26 March 2026. At the latest documented follow-up, the implant-supported and tooth-supported crowns showed stable aesthetic integration. The peri-implant tissues appeared healthy, the buccal contour was maintained, and the interimplant papilla between implants 11 and 12 showed complete fill of the embrasure. The Jemt papilla index improved from score 0 at T1 to score 3 at T2, corresponding to elimination of the visible interimplant black triangle. No clinical evidence of graft necrosis, graft exposure, peri-implant inflammation, prosthetic instability, or loss of the reconstructed papillary volume was documented (**Figure 7, 8**).

Figure 7. Healing and final clinical outcome, frontal view. The final result shows improved buccal contour, stable aesthetic integration, and complete interimplant papilla fill between implants 11 and 12, corresponding to Jemt score 2.

Figure 8. Healing and final clinical outcome, lateral view. The final lateral aspect demonstrates maturation of the buccal soft-tissue contour and integration of the definitive restorations with the peri-implant mucosa, now corresponding to Jemt score 3.

Jemt Papilla Index Assessment

The interimplant papilla between implants 11 and 12 was assessed clinically from standardized frontal intraoral photographs using the Jemt papilla index [9,15]. A score of 0 indicates absence of papilla, 1 indicates less than half papillary fill, 2 indicates at least half papillary fill but incomplete closure of the embrasure, 3 indicates complete papillary fill, and 4 indicates hyperplastic or excessive papillary tissue. In this case, the papilla improved from Jemt score 0 at T1 to Jemt score 3 at T2.

Intraoral Scan and CloudCompare Workflow

Serial full-arch maxillary STL files corresponding to T0, T1, and T2 were imported into CloudCompare v2.14 beta. The datasets were renamed to facilitate identification and manipulation, and different colours were assigned to the three timepoints to improve visual differentiation during superimposition.

Before registration, the datasets were oriented in a patient-based coordinate system. The X axis was standardised to correspond to the sagittal direction of the anterior maxilla, the Z axis to the coronal direction, and the Y axis to the vertical apicocoronal direction. The original datasets were preserved unchanged, and duplicate copies were created for all subsequent manipulations.

An initial manual pre-alignment of T0 with T1 and of T0 with T2 was first performed to bring the full-arch scans into an approximate common position. This preliminary alignment allowed the same anterior region to be segmented consistently across T0, T1, and T2 before final registration.

For registration, the treated anterior segment was excluded from duplicate datasets to prevent the reconstructed area from influencing alignment. The remaining reference datasets therefore included only the stable, non-treated posterior and premolar anatomy. The region from the mesial aspect of tooth 13 to the mesial aspect of tooth 23 was removed, creating trimmed datasets for registration.

Manual point-pair registration was then performed using four homologous landmarks on stable posterior/premolar teeth: the mesiobuccal cusp tip of tooth 17, a reproducible point on the palatal incline of the buccal cusp of tooth 14, a reproducible point on the palatal incline of the buccal cusp of tooth 24, and the mesiobuccal cusp tip of tooth 27. The same T0 dataset was used as the reference for both T0-T1 and T0-T2 registration (**Figure 9**).

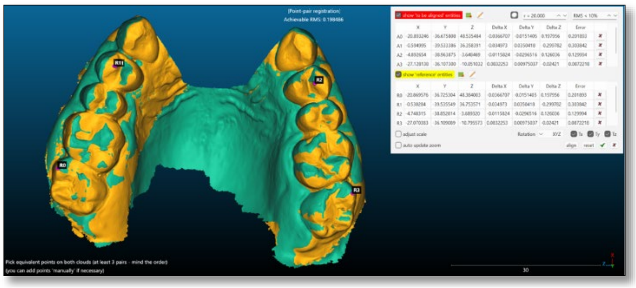

Figure 9. T0-T1 manual point-pair registration after segmentation. CloudCompare view showing the trimmed datasets used for registration after exclusion of the treated anterior region. Four homologous reference points were selected on stable posterior and premolar anatomy to perform the initial landmark-based alignment between T0 and T1. The achievable manual registration RMS was 0.198486 mm.

After manual registration, fine registration was refined with the iterative closest point (ICP) algorithm using the trimmed stable-reference datasets. The final overlap parameter was set at 90%, scale was fixed at 1.0, normals were ignored, and multithread processing was used. The resulting transformation matrices represented alignment based only on stable anatomy and were not influenced by the surgically or prosthetically modified anterior region.

The transformation matrix obtained from the aligned T1 remaining dataset was copied and applied to the corresponding original unsegmented T1 dataset. The same procedure was repeated for T2. In this way, the complete original T1 and T2 scans were brought into the same coordinate system as T0 while preserving the anterior anatomy for subsequent analysis (**Figure 10**).

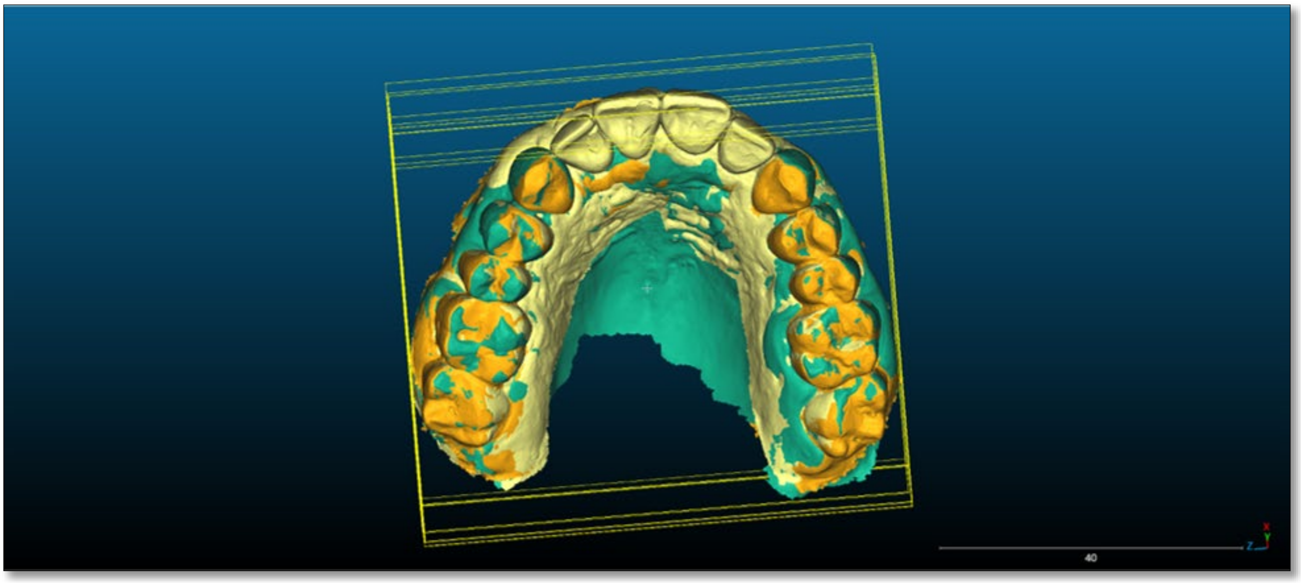

Figure 10. Transformation matrix applied to the original unsegmented dataset. CloudCompare view showing the complete full-arch scan after copy-and-paste application of the alignment matrix obtained from the segmented stable-reference registration. The image demonstrates close overlap of the registered files while preserving the treated anterior region for subsequent surface-distance and 2.5-dimensional surface-change analyses.

After matrix application to the original full-arch datasets, the buccal region of interest (ROI) was segmented for analysis. The buccal ROI extended from the distal aspect of tooth 13 to the distal aspect of tooth 22 and included the reconstructed buccal soft-tissue envelope, including the interimplant embrasure region as part of the broader buccal surface (**Figure 11**).

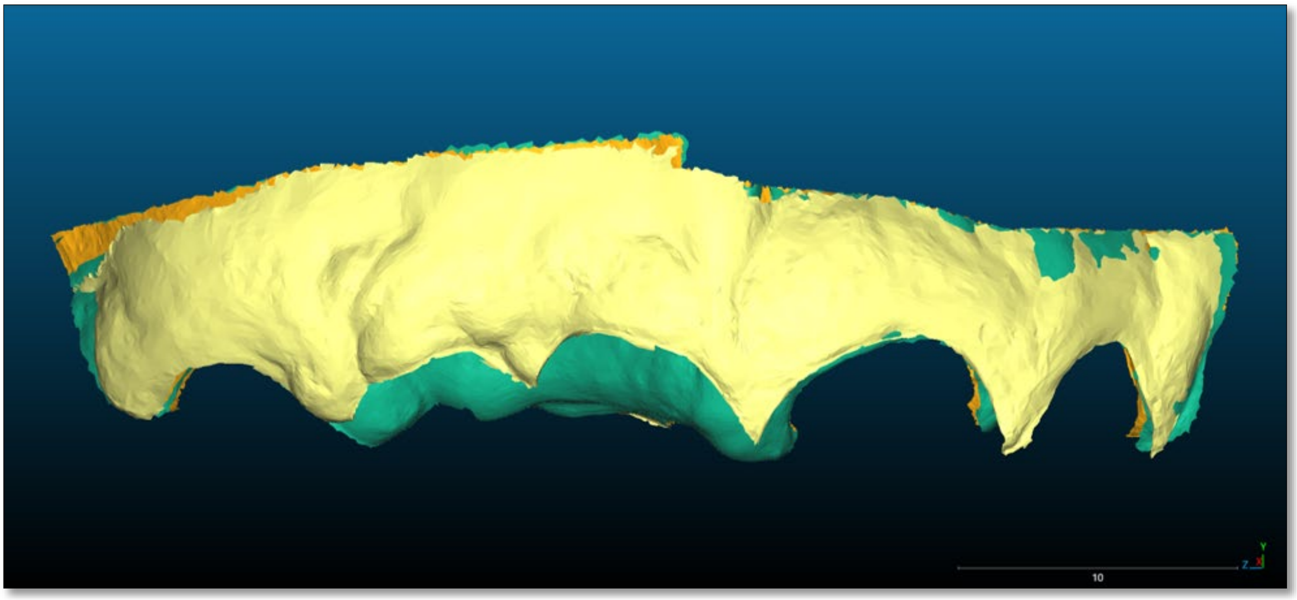

Figure 11. Superimposed segmented buccal regions of interest, frontal view. CloudCompare view showing the T0, T1, and T2 datasets overlapped after registration, with the same buccal ROI segmentation applied to all three timepoints. The ROI extended from the distal aspect of tooth 13 to the distal aspect of tooth 22, allowing subsequent surface-distance and 2.5-dimensional surface-change analyses to compare equivalent anatomical regions across the serial scans.

For directional 2.5-dimensional surface-change analysis, the segmented reference and comparison datasets were converted into point clouds. The earlier timepoint was assigned as the ground/before dataset, and the later registered timepoint was assigned as the ceiling/after dataset. A grid step of 0.100 mm and average cell height were used. Directional 2.5D surface-change indicators were calculated using X, Y, and Z projection directions. The X projection was considered the most clinically relevant as the X axis was aligned with the patient's sagittal dimension. Therefore, changes detected along this projection primarily reflected labial-palatal displacement of the buccal contour in the operated anterior maxillary region, corresponding to the frontal clinical assessment of the reconstructed soft-tissue profile (**Figures 16-18, 21**).

For surface-distance analysis, cloud-to-mesh (C2M) signed-distance calculations were performed for T0-T1, T0-T2, and T1-T2 comparisons using the buccal ROI. C2M signed distances were used to describe the direction of local surface displacement, while C2C absolute distances were used to describe the magnitude of local surface differences. Positive C2M signed distances were defined as outward displacement of the later scan relative to the earlier reference surface, whereas negative values indicated inward displacement. The analysed point-cloud exports were saved as TXT files containing X, Y, and Z coordinates, RGB values, scalar-field distance values, and normal vectors (**Figures 12-15**).

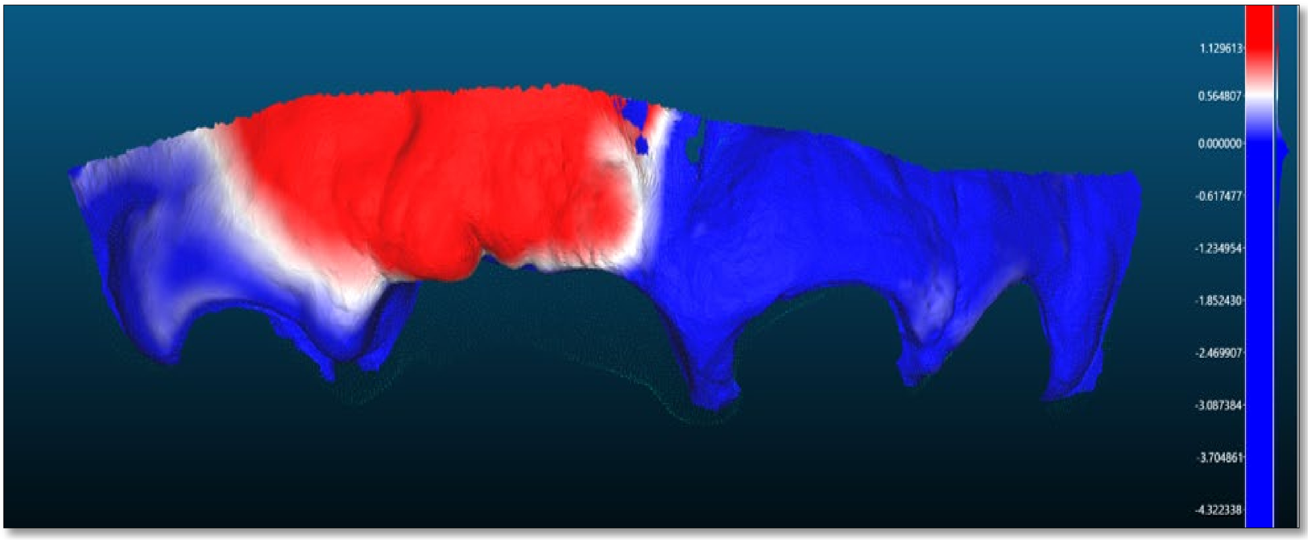

Figure 12. T0-T1 C2M signed-distance map of the segmented buccal ROI, frontal view. CloudCompare blue-white-red heat map showing surface displacement between the baseline scan (T0) and the intermediate scan (T1) within the buccal region of interest. Red areas indicate positive outward displacement of the later scan relative to the earlier reference surface, whereas blue areas indicate negative inward displacement.

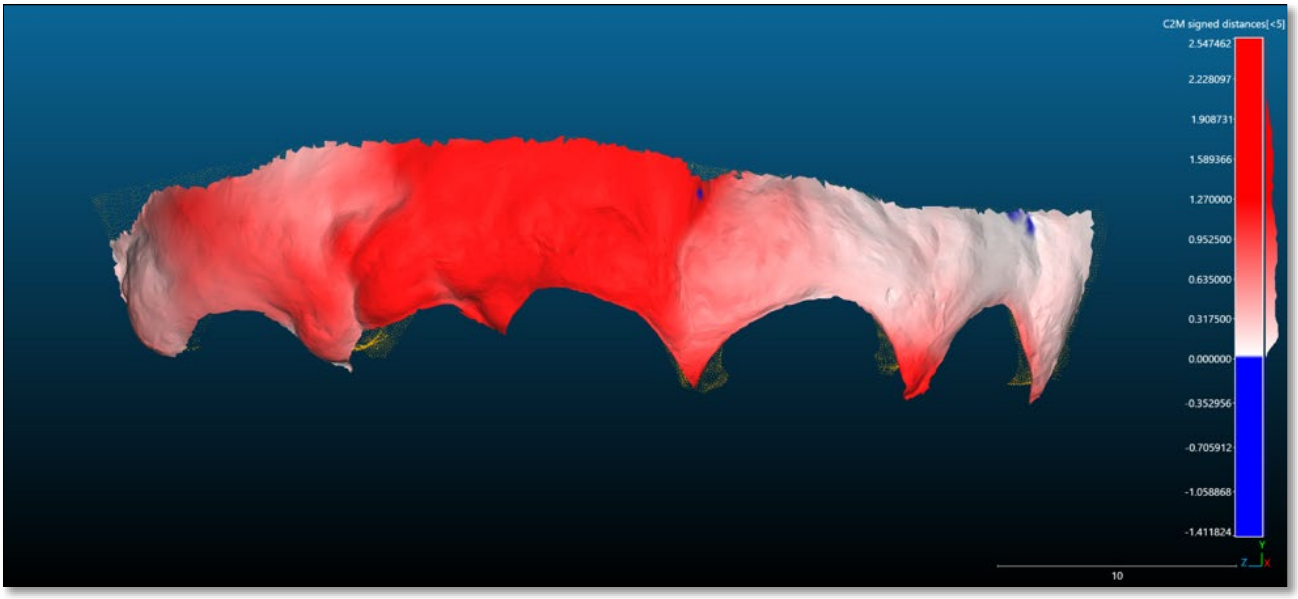

Figure 13. T1-T2 C2M signed-distance map of the segmented buccal ROI, frontal view. CloudCompare blue-white-red heat map showing surface displacement between the intermediate scan (T1) and the final scan (T2) within the buccal region of interest. The predominantly positive displacement pattern indicates post-reconstructive outward surface change of the anterior buccal soft-tissue contour after graft maturation.

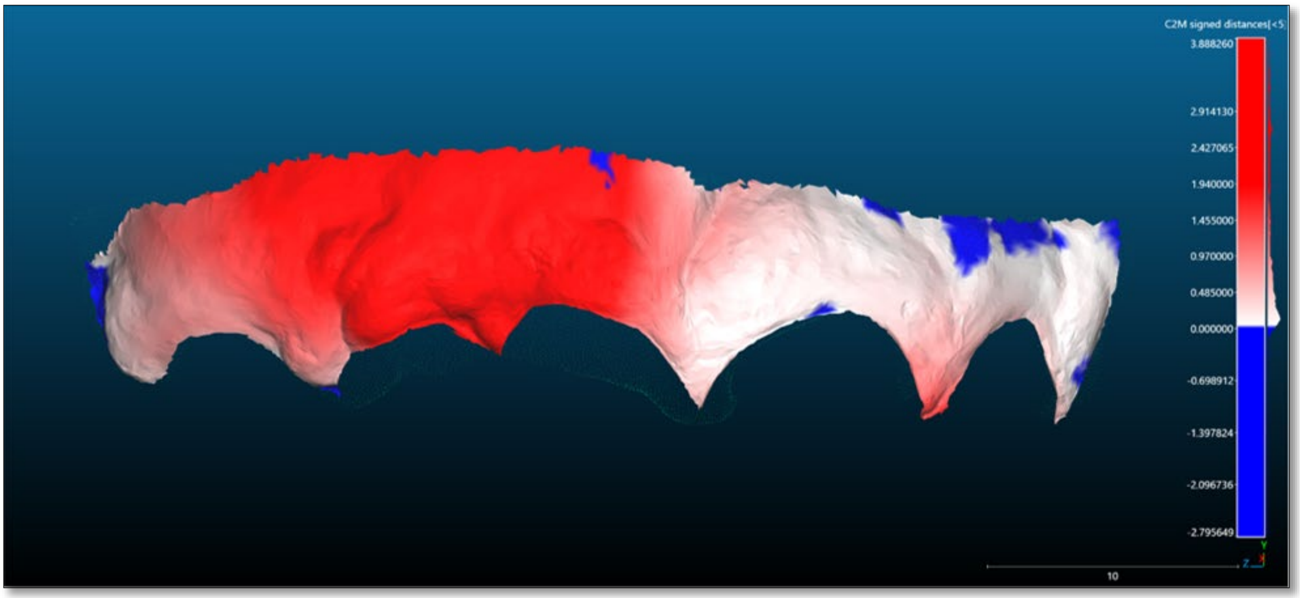

Figure 14. T0-T2 C2M signed-distance map of the segmented buccal ROI, frontal view. CloudCompare blue-white-red heat map showing cumulative surface displacement between the baseline scan (T0) and the final scan (T2) within the buccal region of interest. The predominantly red pattern in the anterior reconstructed area indicates positive outward displacement of the final surface relative to baseline, consistent with cumulative buccal contour gain.

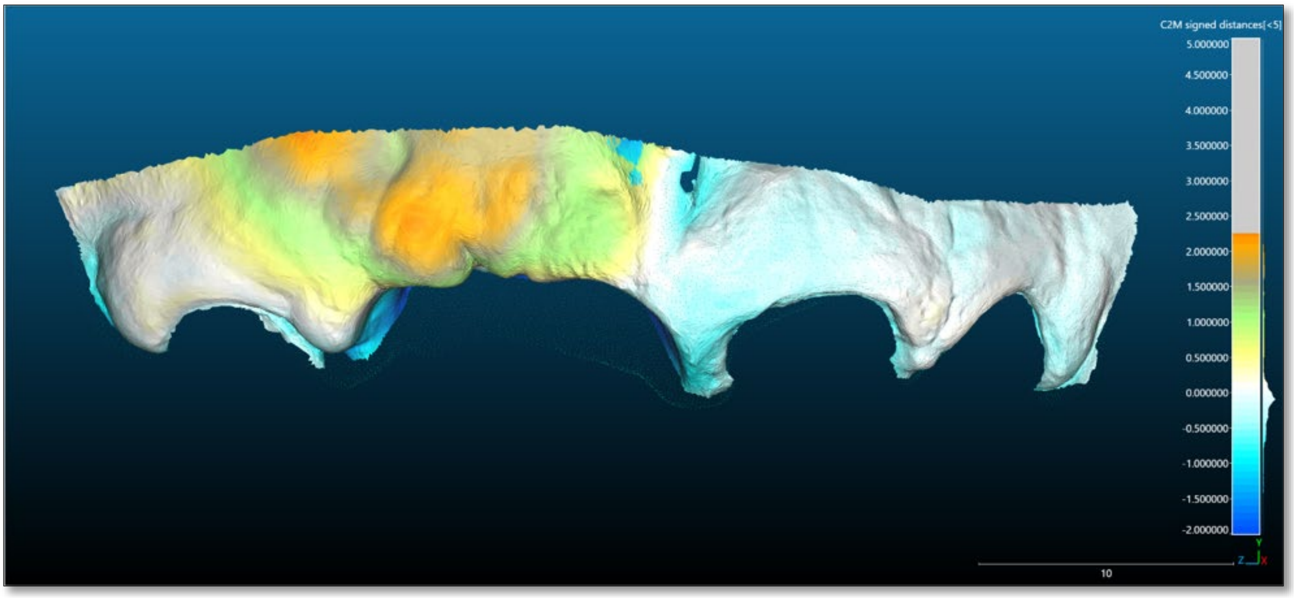

Figure 15. T0-T2 classified C2M signed-distance map of the segmented buccal ROI, frontal view. CloudCompare heat map showing cumulative surface displacement between T0 and T2 using a classified colour scale with 0.5-mm intervals, ranging from -2.0 mm to +5.0 mm. This visualization was used to identify the location and magnitude of buccal surface-contour changes across the reconstructed anterior region.

Registration Results

Directional 2.5D Surface-Change Indicator Results

The 0.100-mm grid step values demonstrated projection-dependent dimensional change. Because the scans were oriented into a patient-based coordinate system before measurement, the X projection was interpreted as the primary buccopalatal indicator of external anterior contour change. The Y and Z projections were retained as directional sensitivity outputs rather than as isolated measures of graft volume.

Table 1. Registration Results (T0: Baseline, T1: Intermediate, T2: Final).

Comparison	Manual point-pair RMS (mm)	Final ICP RMS (mm)	ICP points used	Interpretation
T0-T1	0.198486	0.125312	45,033	Acceptable alignment after registration on stable non-treated anatomy.
T0-T2	0.202457	0.167108	45,201	Acceptable alignment after registration on stable non-treated anatomy.
T1-T2	Not independently registered	Derived from T1 and T2 transformations to T0	Not applicable	Comparison performed after both datasets were transformed into the T0 coordinate system.

Table 2. Directional 2.5D surface-change indicator results for the segmented buccal ROI.

Comparison	X projection net indicator (mm3)	Y projection net indicator (mm3)	Z projection net indicator (mm3)	Interpretation
T0-T1	+23.626	-8.476	+88.597	Mixed early contour redistribution with limited X-direction gain.
T0-T2	+283.495	+0.587	+214.543	Cumulative positive buccal contour change, greatest in the X projection.
T1-T2	+249.337	-3.423	+126.435	Main post-reconstructive buccal gain occurred between T1 and T2.

ROI-Based Buccal C2M Signed-Distance and C2C Absolute-Distance Results

The segmented buccal ROI exports were assessed using C2M signed-distance and C2C absolute-distance scalar fields. C2M signed distance described the direction of surface displacement after registration, whereas C2C absolute distance described the magnitude of local surface difference. The final quantitative analysis was based on the buccal ROI only; no separate papilla ROI file was included in the final results.

Table 3. Descriptive C2M signed-distance statistics for the segmented buccal ROI.

Comparison	n points	Mean signed (mm)	Median signed (mm)	SD (mm)	Min-Max (mm)	P5-P95 (mm)	% positive	>+1.0 mm	>+2.0 mm
T0-T1	49,946	-0.168	-0.080	1.323	-4.917 to +2.243	-3.030 to +1.801	42.22%	18.15%	1.89%
T0-T2	49,994	+1.281	+0.896	1.153	-2.795 to +3.884	+0.026 to +3.360	96.33%	47.59%	29.23%
T1-T2	49,974	+0.896	+0.837	0.536	-1.460 to +2.444	+0.147 to +1.804	99.95%	38.82%	0.74%

The cumulative T0-T2 comparison showed predominantly positive buccal surface displacement, with a mean signed distance of +1.281 mm, a median of +0.896 mm, and 96.33% of sampled points showing positive values. The T1-T2 comparison was also predominantly positive, with a mean signed distance of +0.896 mm and 99.95% positive values, indicating that most of the measurable buccal contour gain occurred after the soft-tissue reconstruction phase. The T0-T1 comparison showed mixed displacement, with a slightly negative mean signed distance (-0.168 mm) and 42.22% positive values, consistent with early contour redistribution before the definitive post-grafting maturation interval.

RESULTS

Clinically, the staged surgical-prosthetic protocol restored anterior dental continuity and improved the peri-implant tissue architecture after traumatic loss of teeth 11 and 12 and associated buccal plate damage. The most clinically relevant aesthetic change was the conversion of the interimplant papilla between implants 11 and 12 from Jemt score 0 at T1 to Jemt score 3 at T2, with elimination of the visible black triangle.

The revised IOS registration workflow achieved final ICP RMS values of 0.125312 mm for T0-T1 and 0.167108 mm for T0-T2 after exclusion of the treated anterior region from the registration dataset. The T1-T2 comparison was not independently registered; it was derived after T1 and T2 were independently transformed into the T0 coordinate system using their respective stable-reference registrations (**Figures 9, 10**).

The directional 2.5D analysis confirmed that the measured surface-change indicators depended on projection direction. In the clinically relevant X projection, the segmented buccal ROI showed net positive indicators of +23.626 mm3 for T0-T1, +283.495 mm3 for T0-T2, and +249.337 mm3 for T1-T2. These values indicate that the main measurable buccopalatal contour gain occurred between T1 and T2, after soft-tissue reconstruction (**Figures 16-18, 21**).

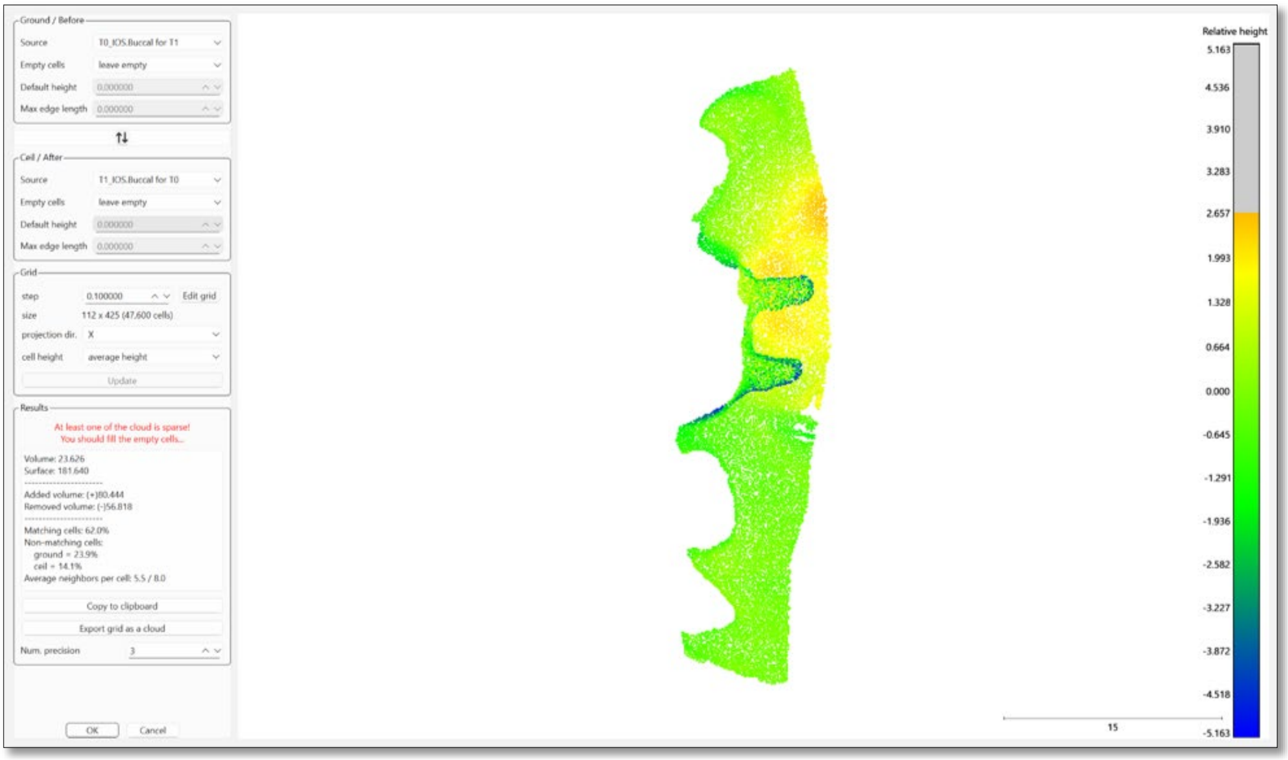

Figure 16. T0-T1 directional 2.5D surface-change assessment in the X projection. CloudCompare volume-calculation window showing the comparison between the segmented buccal ROI at T0 and T1 using the X-axis projection, a 0.100-mm grid step, and average cell height. The net X-projection surface-change indicator was +23.626 mm3, representing limited early buccopalatal contour change before the soft-tissue reconstruction phase.

Figure 17. T1-T2 directional 2.5D surface-change assessment in the X projection. CloudCompare volume-calculation window showing the comparison between the segmented buccal ROI at T1 and T2 using the X-axis projection, a 0.100-mm grid step, and average cell height. The net X-projection surface-change indicator was +249.337 mm3, demonstrating that the main post-reconstructive buccopalatal contour gain occurred between the intermediate and final scans.

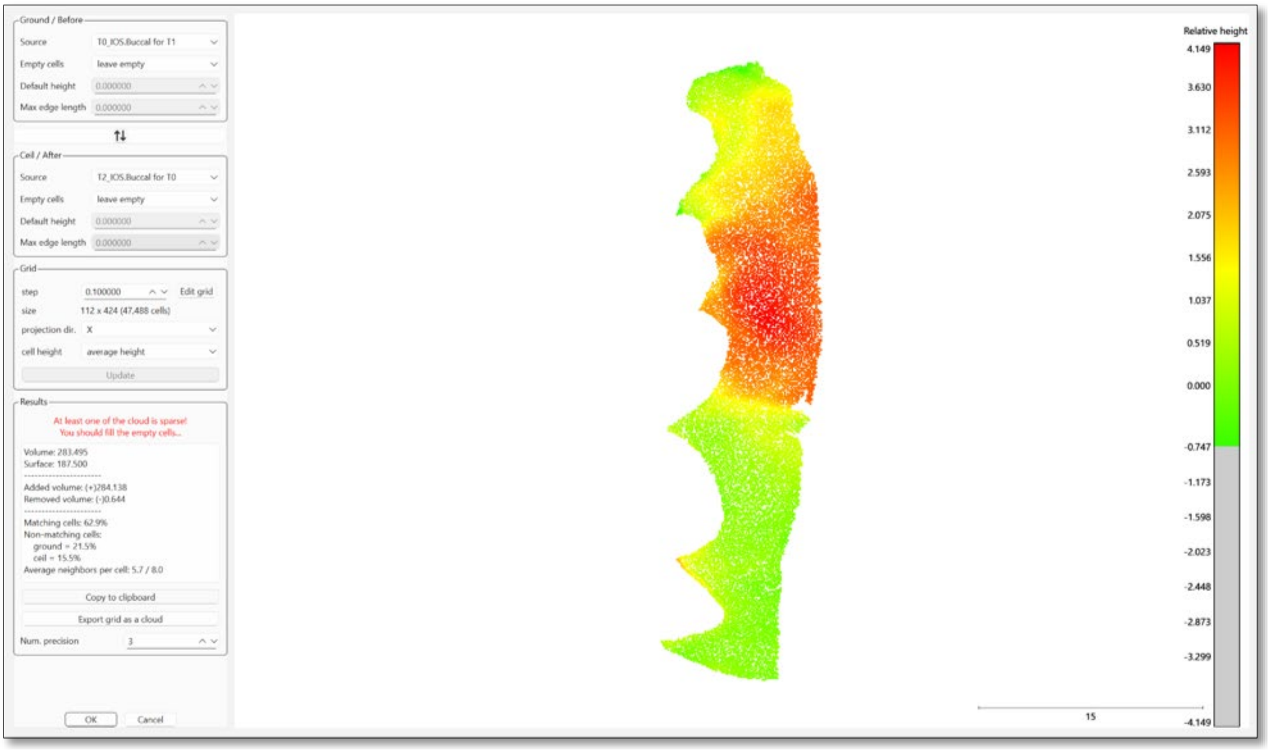

Figure 18. T0-T2 directional 2.5D surface-change assessment in the X projection. CloudCompare volume-calculation window showing the comparison between the segmented buccal ROI at T0 and T2 using the X-axis projection, a 0.100-mm grid step, and average cell height. The net X-projection surface-change indicator was +283.495 mm3, representing the cumulative buccopalatal contour gain from baseline to the final follow-up scan.

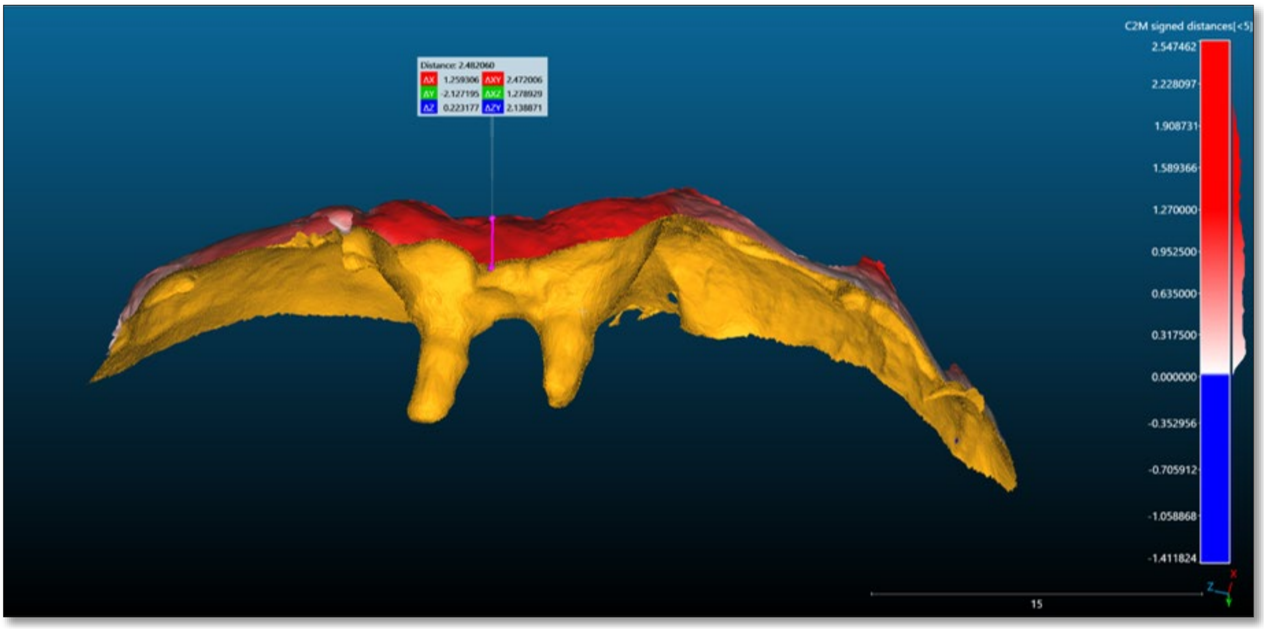

Figure 19. Superimposed T1 and T2 meshes of the segmented buccal ROI, palatal-internal oblique view. CloudCompare view showing the registered superimposed meshes from the intermediate (T1) and final (T2) scans, viewed from the internal/palatal aspect of the segmented region. A linear measurement at the interimplant papilla between implants 11 and 12 demonstrated an approximately 2.48-mm vertical difference, illustrating the marked papillary height gain that occurred during the post-reconstructive interval.

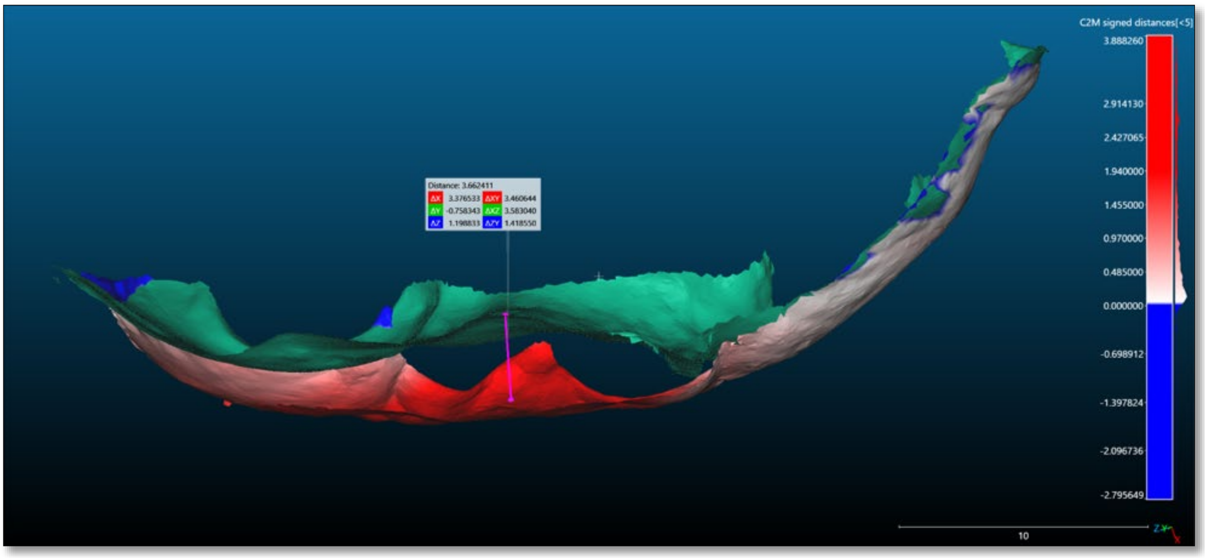

Figure 20. Superimposed T0 and T2 meshes showing buccal contour change in the interimplant region. CloudCompare view of the registered segmented buccal ROI comparing the baseline (T0) and final (T2) scans from the buccal aspect. A linear measurement in the buccal soft-tissue region between implants 11 and 12 demonstrated an approximately 3.66-mm surface difference, illustrating the cumulative buccal contour gain in this area rather than vertical papillary height change.

C2M signed-distance analysis of the buccal ROI supported the 2.5D findings. The T0-T2 comparison showed a mean signed distance of +1.281 mm and a median of +0.896 mm, with 96.33% of sampled points showing positive displacement. The T1-T2 comparison showed a mean signed distance of +0.896 mm and a median of +0.837 mm, with 99.95% positive values. By contrast, the T0-T1 interval showed mixed redistribution, with a mean signed distance of -0.168 mm and 42.22% positive values (**Figures 12-15**).

The signed-distance maps demonstrated that the most evident positive displacement was concentrated in the reconstructed anterior buccal region, including the interimplant embrasure as part of the broader buccal ROI (**Figures 12-15**). The superimposed mesh views also illustrated local papillary and buccal contour differences (**Figures 19, 20**). These digital findings should be interpreted as external surface-contour documentation rather than as direct biological measurement of graft volume.

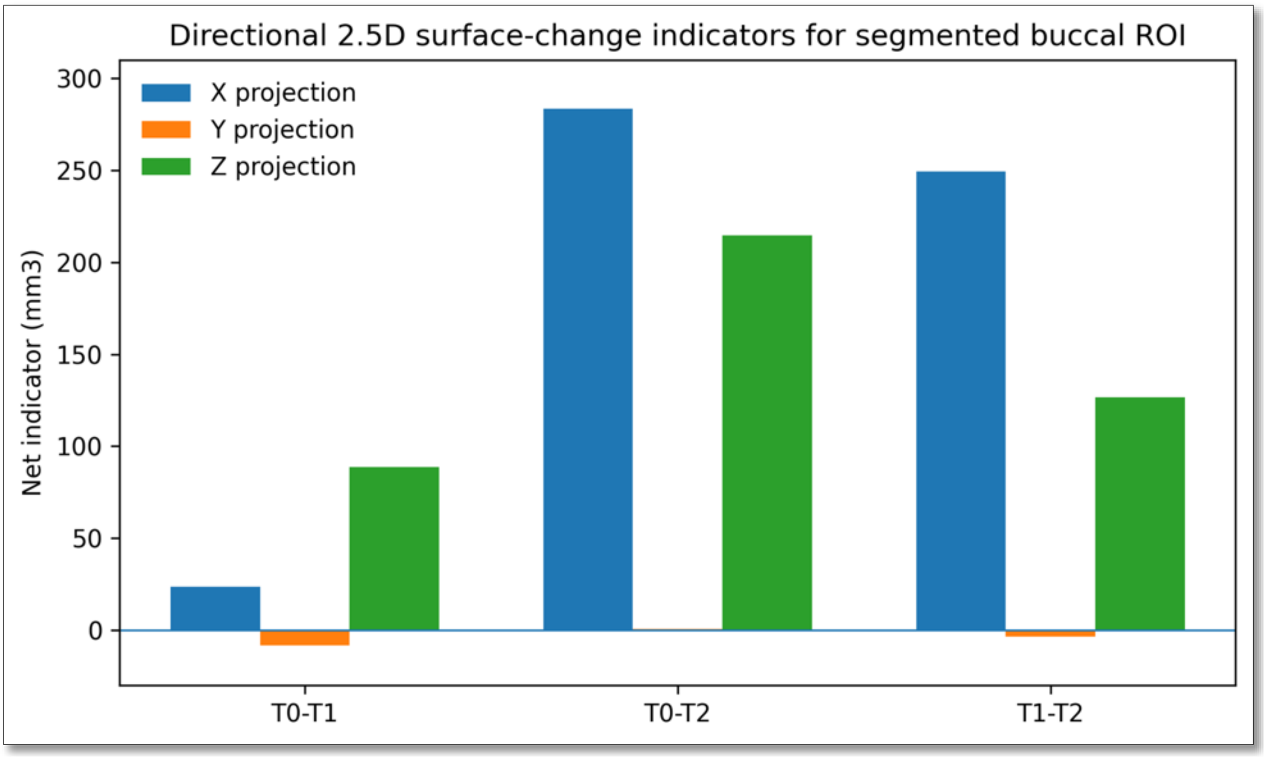

Figure 21. Directional 2.5-dimensional surface-change indicators. Summary chart of X, Y, and Z projection values for T0-T1, T0-T2, and T1-T2 comparisons at a 0.10-mm grid step, demonstrating projection-dependent surface change of the segmented buccal ROI.

DISCUSSION

This report presents a staged surgical-prosthetic alternative for managing a difficult interimplant papilla deficiency after severe anterior maxillary trauma. The clinical relevance of the case lies in the combination of adjacent implants, traumatic buccal plate loss, soft-tissue collapse, and a persistent black triangle after provisional conditioning and definitive crown delivery. In this situation, papilla reconstruction depended on coordinated prosthetic and surgical decisions rather than on grafting alone.

The narrowed definitive crown contours were important because they created space for graft placement and reduced compression of the peri-implant mucosa. Prosthetic emergence profile management is an established component of aesthetic-zone implant rehabilitation, and provisional or definitive contours can influence soft-tissue architecture.[6,7] In the present case, the definitive restorations were intentionally modified before soft-tissue reconstruction so that the pediculated graft could occupy a protected interimplant space.

The improvement from Jemt score 0 to Jemt score 3 is clinically significant. It indicates that the interimplant papilla changed from complete absence of papillary fill with a visible black triangle to complete fill of the interimplant embrasure. In a region where papilla reconstruction between adjacent implants is considered difficult, this outcome supports the clinical value of the combined prosthetic-space creation, tunneled pediculated connective tissue graft, and buccal connective tissue augmentation.

The surgical approach attempted to preserve blood supply and tissue continuity. The tunnel design avoided vertical releasing incisions in the aesthetic zone and preserved the papillary envelope. The palatal graft remained attached by a mesial pedicle, which may have improved early vascular support compared with a completely free graft. The additional free connective tissue graft was used because correction of the papilla alone would not have restored the buccal convexity. In aesthetic-zone implant therapy, the visual appearance of the papilla is influenced by the surrounding buccal contour; therefore, both defects were treated in the same reconstructive phase.

The second contribution of this report is the digital workflow. The IOS and CloudCompare protocol provides a practical way to document changes in external soft-tissue contour without additional radiation exposure. The most important methodological point is that the treated anterior segment was removed before registration; therefore, alignment was driven by stable posterior and premolar anatomy rather than by the changing reconstructed region.

The directional 2.5D findings should be interpreted carefully. The anterior maxilla is not a flat surface, and 2.5-dimensional calculation is affected by projection direction. For this reason, X, Y, and Z projection values were reported separately. After patient-oriented axis standardisation, the X projection was considered the most clinically relevant direction for buccopalatal contour change in the anterior maxilla.

This clinical report has limitations. It describes one patient, and the IOS method was not validated against another volumetric modality. The workflow documents external surface change and cannot distinguish the biological contribution of graft tissue, mucosal maturation, prosthetic contour, inflammation, or scan-related artefacts. Although the interimplant papilla improved clinically from Jemt score 0 to Jemt score 3, the final quantitative analysis was intentionally limited to the broader buccal ROI and should not be interpreted as an isolated papilla-volume measurement.

SUMMARY AND CONCLUSION

A traumatic anterior maxillary defect involving avulsion of teeth 11 and 12, crown fractures of teeth 21 and 22, and buccal plate fracture was rehabilitated with a staged surgical-prosthetic protocol. The treatment combined endodontic and restorative management, implant placement, definitive prosthetic contour modification, a tunneled palatal pediculated connective tissue graft for papilla reconstruction, and a second connective tissue graft for broader buccal contour augmentation.

Serial intraoral scanning and CloudCompare analysis documented the dimensional changes. Stable non-treated posterior and premolar anatomy was used for registration after excluding the treated anterior region, and the resulting transformation matrices were applied to the corresponding full-arch datasets before buccal ROI segmentation. The final quantitative analysis was based on the segmented buccal ROI from the distal aspect of tooth 13 to the distal aspect of tooth 22.

At follow-up, the interimplant papilla between implants 11 and 12 improved from Jemt score 0 to Jemt score 3, the visible black triangle was eliminated, the buccal contour was improved, and the restorations remained clinically stable. The IOS analysis documented positive cumulative buccal surface displacement from T0 to T2, supporting intraoral scanning as a useful non-ionising method for longitudinal documentation of peri-implant soft-tissue contour change.

INTERPRETATION OF THE CASE

The most clinically important finding is not only a measured surface change, but the conversion of an absent interimplant papilla to complete papillary fill: Jemt score 0 at T1 to Jemt score 3 at T2.

The prosthetic decision to narrow the transmucosal crown contours appears to have been essential because it created a protected space into which the pediculated connective tissue graft could be positioned and mature.

The tunneled pediculated palatal graft addressed the interimplant papilla deficiency, while the second connective tissue graft addressed the broader buccal collapse. This supports the idea that papilla reconstruction and buccal contour augmentation are related but distinct objectives.

The IOS workflow provides useful non-ionising documentation of external surface changes, but it should be interpreted as surface contour documentation, not as a direct measurement of bone gain or isolated biological graft volume.

The 2.5D analysis demonstrated projection-dependent dimensional change; therefore, the X, Y, and Z outputs should be reported transparently, with the X projection interpreted as the main buccopalatal indicator after patient-oriented axis standardisation.

The case is best interpreted as a clinical proof-of-concept for a combined surgical-prosthetic strategy, not as evidence that the technique is predictably reproducible in all patients.

PATIENT CONSENT AND ETHICAL STATEMENT

Written informed consent was obtained from the patient for treatment and for publication of anonymized clinical photographs, intraoral scans, digital images, and clinical information. Images used for publication were cropped or anonymized to minimize patient identification.

CONFLICT OF INTEREST STATEMENT

The authors declare no conflicts of interest related to this clinical report.

FUNDING STATEMENT

No external funding was received for this clinical report.

DATA AVAILABILITY STATEMENT

Clinical photographs, intraoral scan files, CloudCompare exports, buccal ROI C2M signed-distance data, C2C absolute-distance data, and supporting documentation are available from the corresponding author upon reasonable request, subject to patient confidentiality and consent restrictions.

AUTHOR CONTRIBUTIONS

Bruno Viana Reis was responsible for conceptualization, diagnosis, treatment planning, endodontic treatment of teeth 21 and 22, fibre-post reconstruction, tooth preparation, prosthetic planning, clinical prosthetic execution, implant planning, case documentation, manuscript drafting, and final manuscript review. Victor Vidigal was responsible for the periodontal surgical procedure for interimplant papilla reconstruction, including soft-tissue graft planning, tunnel preparation, pediculated connective tissue graft rotation, buccal soft-tissue augmentation, clinical documentation, manuscript review, and approval of the final manuscript. Fillipe Marcone dos Santos Dutra was responsible for digital prosthetic planning, CAD/CAM laboratory workflow, design and fabrication of provisional restorations, and fabrication of the definitive zirconia implant-supported crowns. He also contributed to technical documentation, manuscript review, and approval of the final manuscript. Renan Lana Devita contributed to case documentation organization, manuscript structuring, critical manuscript review, intellectual revision of the final text, and approval of the final manuscript. All authors reviewed and approved the final version before submission.

REFERENCES

1. Tarnow DP, Magner AW, Fletcher P. The effect of the distance from the contact point to the crest of bone on the presence or absence of the interproximal dental papilla. J Periodontol.1992;63(12):995-996. doi:10.1902/jop.1992.63.12.995.

2. Tarnow DP, Cho SC, Wallace SS. The effect of inter-implant distance on the height of inter-implant bone crest. J Periodontol.2000;71(4):546-549. doi:10.1902/jop.2000.71.4.546.

3. Thoma DS, Buranawat B, Hammerle CHF, Held U, Jung RE. Efficacy of soft tissue augmentation around dental implants and in partially edentulous areas: a systematic review. J Clin Periodontol. 2014;41 Suppl 15:S77-S91. doi:10.1111/jcpe.12220.

4. Seyssens L, De Lat L, Cosyn J. Immediate implant placement with or without connective tissue graft: a systematic review and meta-analysis. J Clin Periodontol. 2021;48(2):284-301. doi:10.1111/jcpe.13397.

5. Mangano F, Gandolfi A, Luongo G, Logozzo S. Intraoral scanners in dentistry: a review of the current literature. BMC Oral Health. 2017;17:149. doi:10.1186/s12903-017-0442-x.

6. Wittneben JG, Buser D, Belser UC, Bragger U. Peri-implant soft tissue conditioning with provisional restorations in the esthetic zone: the dynamic compression technique. Int J Periodontics Restorative Dent. 2013;33(4):447-455. doi:10.11607/prd.1268.

7. Zucchelli G, Mazzotti C, Mounssif I, Mele M, Stefanini M, Montebugnoli L. A novel surgical-prosthetic approach for soft tissue dehiscence coverage around single implant. Clin Oral Implants Res. 2013;24(9):957-962. doi:10.1111/clr.12003.

8. Salama H, Salama MA, Garber D, Adar P. The interproximal height of bone: a guidepost to predictable aesthetic strategies and soft tissue contours in anterior tooth replacement. Pract Periodontics Aesthet Dent. 1998;10(9):1131-1141.

9. Jemt T. Regeneration of gingival papillae after single-implant treatment. Int J Periodontics Restorative Dent. 1997;17(4):326-333.

10. Ioannou AL, Kotsakis GA, McHale MG, Lareau DE, Hinrichs JE, Romanos GE. Soft tissue surgical procedures for optimizing anterior implant esthetics. Int J Dent. 2015;2015:740764. doi:10.1155/2015/740764.

11. Patel M, Guni A, Nibali L, Garcia-Sanchez R. Interdental papilla reconstruction: a systematic review. Clin Oral Investig. 2024;28(1):101. doi:10.1007/s00784-023-05409-0.

12. Gagnier JJ, Kienle G, Altman DG, Moher D, Sox H, Riley D; CARE Group. The CARE guidelines: consensus-based clinical case reporting guideline development. Glob Adv Health Med. 2013;2(5):38-43. doi:10.7453/gahmj.2013.008.

13. Jung RE, Becker K, Bienz SP, Dahlin C, Donos N, Hammächer C, Iglhaut G, Liñares A, Ortiz-Vigón A, Sanchez N, Sanz-Sánchez I, Thoma DS, Valles C, Weng D, Nart J. Effect of peri-implant mucosal thickness on esthetic outcomes and the efficacy of soft tissue augmentation procedures: Consensus report of group 2 of the SEPA/DGI/OF workshop. Clin Oral Implants Res. 2022;33(Suppl 23):100-108. doi:10.1111/clr.13955.

14. Zuhr O, Rebele SF, Schneider D, Jung RE, Hürzeler MB. Surgery without papilla incision: tunneling flap procedures in plastic periodontal and implant surgery. Periodontol 2000. 2018;77(1):11-34. doi:10.1111/prd.12214.

15. Fürhauser R, Florescu D, Benesch T, Haas R, Mailath G, Watzek G. Evaluation of soft tissue around single-tooth implant crowns: the pink esthetic score. Clin Oral Implants Res. 2005;16(6):639-644. doi:10.1111/j.1600-0501.2005.01193.x.

16. Avila-Ortiz G, Gonzalez-Martin O, Couso-Queiruga E, Wang HL. The peri-implant phenotype. J Periodontol. 2020;91(3):283-288. doi:10.1002/JPER.19-0566.

17. Andersson L, Andreasen JO, Covington P, et al. International Association of Dental Traumatology guidelines for the management of traumatic dental injuries: 2. Avulsion of permanent teeth. Dent Traumatol. 2012;28(2):88-96. doi:10.1111/j.1600-9657.2012.01125.x.

18. Charalambous P, et al. A technique for comparing volumetric changes in soft tissue or in dental hard tissue between 2 scans recorded by using any IOS. J Prosthet Dent. 2024. doi:10.1016/j.prosdent.2024.03.018.